Cancer-Induced Immunosuppression: IL-18-Elicited Immunoablative NK Cells

Article *in* Cancer Research · March 2012

Impact Factor: 9.33 · DOI: 10.1158/0008-5472.CAN-11-3379 · Source: PubMed

Cancer Research

Cancer-Induced Immunosuppression: IL-18–Elicited Immunoablative NK Cells

Magali Terme, Evelyn Ullrich, Laetitia Aymeric, et al.

Cancer Res 2012;72:2757-2767. Published OnlineFirst March 16, 2012.

Published OnlineFirst March 16, 2012; DOI:10.1158/0008-5472.CAN-11-3379

Microenvironment and Immunology

Cancer Research

Cancer-Induced Immunosuppression: IL-18–Elicited Immunoablative NK Cells

Magali Terme[1,2,5], Evelyn Ullrich[1,2,10], Laetitia Aymeric[1,2], Kathrin Meinhardt[10], Jérôme D. Coudert[11], Mélanie Desbois[1,2], François Ghiringhelli[1,2,4], Sophie Viaud[1,2], Bernard Ryffel[12], Hideo Yagita[13], Lieping Chen[14], Salaheddine Mécheri[7], Gilles Kaplanski[15], Armelle Prévost-Blondel[6,8], Masashi Kato[16], Joachim L. Schultze[17], Eric Tartour[5], Guido Kroemer[1,3,9], Mariapia Degli-Esposti[11], Nathalie Chaput[1,4], and Laurence Zitvogel[1,2,4]

Abstract

During cancer development, a number of regulatory cell subsets and immunosuppressive cytokines subvert adaptive immune responses. Although it has been shown that tumor-derived interleukin (IL)-18 participates in the PD-1–dependent tumor progression in NK cell–controlled cancers, the mechanistic cues underlying this immunosuppression remain unknown. Here, we show that IL-18 converts a subset of Kit^- ($CD11b^-$) into Kit^+ natural killer (NK) cells, which accumulate in all lymphoid organs of tumor bearers and mediate immunoablative functions. Kit^+ NK cells overexpressed B7-H1/PD-L1, a ligand for PD-1. The adoptive transfer of Kit^+ NK cells promoted tumor growth in two pulmonary metastases tumor models and significantly reduced the dendritic and NK cell pools residing in lymphoid organs in a B7-H1–dependent manner. Neutralization of IL-18 by RNA interference in tumors or systemically by IL-18–binding protein dramatically reduced the accumulation of Kit^+CD11b^- NK cells in tumor bearers. Together, our findings show that IL-18 produced by tumor cells elicits Kit^+CD11b^- NK cells endowed with B7-H1–dependent immunoablative functions in mice. *Cancer Res; 72(11); 2757–67. ©2012 AACR.*

Introduction

Tumor progression subverts the adaptive arm of antitumor immune responses, either directly by compromising T-cell functions or indirectly by inhibiting antigen-presenting cells. Tumor-infiltrating dendritic cells (DC)/myeloid suppressor cells tend to mediate metabolic immunosuppressive effects and promote the generation and local accumulation of suppressive regulatory T cells or Tr1 $CD4^+$ T cells. Tumor-associated regulatory T cells efficiently inhibit $CD4^+$ T-cell–dependent immune responses and suppress the proliferation and IFNγ production of antigen-experienced $CD8^+$ T cells (1, 2). Interleukin (IL)-10–producing natural killer (NK) cells can also dampen IL-12–dependent immune responses during systemic infections (3). Nonetheless, the clinical relevance and the molecular mechanisms underlying the concept of regulatory NK cells have remained largely unclear (4).

Driven by clinical observations associating high serum levels of IL-18 and NK cell defects (5, 6) as well as the facilitating role of tumor-derived IL-18 in melanoma metastases (7, 8), we investigated the potential immunosuppressive effects of IL-18 in NK cell–controlled tumors (9, 10). We recently reported that low dosing of exogenous IL-18 or tumor-derived IL-18 promoted the dissemination of B16F10 and CT26 metastases in a PD-1–dependent manner (11). However, the precise mechanisms accounting for the IL-18/PD-1 immunosuppressive axis in these NK cell–controlled tumor models were not studied in this report.

Now, we show that IL-18 secreted by tumor cells could convert conventional $Kit^-CD27^+CD11b^-$ NK cells into Kit^+ NK cells with immunosuppressive characteristics. Kit^+CD11b^- NK cells express high levels of B7-H1/PD-L1, which contribute to partial elimination of lymph node DCs, thereby affecting the homeostasis of mature NK cells in a B7-H1–dependent manner. Depletion or neutralization of IL-18

Authors' Affiliations: [1]Institut Gustave Roussy , Villejuif; [2]INSERM, U1015; [3]INSERM, U848;[4]Center of Clinical Investigations CBT507, Biotherapy, Villejuif; [5]INSERM U970, PARCC (Paris Cardiovascular Research Center), Université Paris-Descartes, Sorbonne Paris Cité; [6]Institut Cochin, Université Paris Descartes, CNRS (UMR 8104); [7]Unité de Biologie des Interactions Hôte-Parasite, Institut Pasteur, Paris; [8]INSERM, U1016; [9]Faculté Paris Sud-Université Paris XI, Paris, France; [10]Department of Internal Medicine 5, Hematology and Oncology, University of Erlangen-Nürnberg Erlangen, Germany; [11]Immunology and Virology Program, Centre for Ophthalmology and Visual Science, The University of Western Australia; Australia & Centre for Experimental Immunology, Lions Eye Institute, Nedlands, Western Australia, Australia; [12]CNRS, IEM 2815, Institut Transgénose, Orléans, France; [13]Department of Immunology, Juntendo University School of Medicine, Tokyo, Japan; [14]Johns Hopkins University School of Medicine, The Sidney Kimmel Comprehensive Cancer Center, Baltimore, Maryland; [15]Service de Médecine Interne, Hôpital de la Conception, Marseille, France; [16]Unit of Environmental Health Sciences, Department of Biomedical Sciences, College of Life and Health Sciences, Chubu University, Aichi, Japan; and [17]Laboratory for Genomics and Immunoregulation, LIMES, University of Bonn, Bonn, Germany

Note: Supplementary data for this article are available at Cancer Research Online (http://cancerres.aacrjournals.org/).

M. Terme, E. Ullrich, and L. Aymeric contributed equally to this work.

Corresponding Author: Laurence Zitvogel, INSERM U1015, Institut Gustave Roussy, 39, rue Camille Desmoulins, F-94805 Villejuif, France. Phone: 33-1-42-11-50-41; Fax: 33-1-42-11-60-94; E-mail: zitvogel@igr.fr

doi: 10.1158/0008-5472.CAN-11-3379

Published OnlineFirst March 16, 2012; DOI:10.1158/0008-5472.CAN-11-3379

stimulates tumor surveillance mediated by Kit$^-$ NK cells by preventing the accumulation of Kit$^+$CD11b$^-$ immunoablative NK cells.

Materials and Methods

Mice and tumors

Female C57Bl/6 or BALB/c mice were obtained from Charles River Laboratories, and the Centre d'Elevage Janvier (Le Genest-St-Isle, France). C57Bl/6 nude mice were purchased from Taconic. Myeloid differentiation primary response protein (MyD88)$^{-/-}$ and IL-18 receptor (IL-18R)$\alpha^{-/-}$ mice backcrossed on a C57Bl/6 background were kindly provided by B. Ryffel (CDTA, Orléans, France). W/Wsh mice were kindly provided by S. Mécheri (Institut Pasteur, Paris, France). RET$^{+/-}$ mice were obtained from A. Prévost-Blondel (Institut Cochin, Paris, France) with the permission of Prof. M. Kato (Chubu University, Aichi, Japan). All animals were maintained in Institut Gustave Roussy (Villejuif, France) animal facilities according to the Animal Experimental Ethics Committee Guidelines. B16F10 and CT26 tumor cells were obtained from American Type Culture Collection.

Cytokines and antibodies

Recombinant murine IL-18 and IL-12 were purchased from R&D Systems. For *in vivo* experiments, endotoxin-free bovine serum albumin (BSA)-free rmIL-18 was used (R&D Systems). Rhu IL-2 was purchased from Chiron Corp. Anti-B7-H1 (MIH5) hybridoma was purchased from eBioscience and a second anti-B7-H1 neutralizing antibody (clone 10B5) was provided by L. Chen (Johns Hopkins University School of Medicine, Baltimore, MD; ref. 12). Monoclonal antibodies (purchased from Becton Dickinson Pharmingen, eBioscience, and R&D Systems) to the following mouse antigens were conjugated to fluorescein isothiocyanate (FITC), phycoerythrin (PE), PerCP, allophycocyanin (APC), Pacific Blue, or biotin: NK1.1 (PK136), CD49b (DX5), CD3 (145-2C11), CD117 (2B8 or ACK2), CD27 (LG-3A10), CD11b (M1/70), CD127 (A7R34), NKG2A (16A11), CXCR3 (220803), CD178 (MFL3), B7-H1 (MIH5), PD-1 (J43), CD86 (GL-1), I-Ab (AF6-120.1), and CD11c (HL3). Stained cells were analyzed with FACSCalibur or LSRII cytofluorometers using FACS Diva Software (Becton Dickinson), CellQuest Pro Software (Becton Dickinson), or FlowJo Software (TreeStar).

In vivo IL-18 neutralization

IL-18–binding protein (IL-18BP) was kindly provided by Prof. C. Dinarello (University of Colorado Denver, Denver, CO; ref. 13). At day 0, 3×10^5 B16F10 or CT26 tumor cells were injected i.v. into C57Bl/6 or BALB/c mice. Mice received 20 μg of IL-18BP or saline buffer alone i.p. daily from days 0 to 8. The quantification of lymph nodes and splenic Kit$^+$ NK cells and pulmonary metastases number was conducted on day 9.

Purification of Kit$^+$ NK cells

Splenocytes from C57Bl/6 mice were enriched in NK cells (CD3$^-$NK1.1$^+$) by a magnetic separation using NK cell Isolation Kit (Miltenyi Biotec). Then 2 different protocols were used: (i) enriched NK cells were subjected to another magnetic separation with CD117 microbeads to isolate Kit$^+$ NK (CD117$^+$) and Kit$^-$ NK cells (CD117$^-$); and (ii) enriched NK cells were stained with FITC-conjugated anti-CD117 and PE-conjugated anti-NK1.1 monoclonal antibodies to allow sorting on a FACS Vantage instrument (BD Biosciences) or a Mo-Flo instrument (DAKO). The purity of the CD3$^-$NK1.1$^+$CD117$^+$ and CD3$^-$NK1.1$^+$CD117$^-$ cell subset was approximately 70% after magnetic separation and 98% after cell sorting. Three subsets of Kit$^+$ NK cells were also separated according to their CD27 and CD11b expression using FITC anti-CD3, PE anti-CD27, PE-Cy7 anti-NK1.1, APC anti-CD117, and Pacific Blue anti-CD11b antibody to allow cell sorting on a Mo-Flo instrument.

siRNA transfections of tumor cells

B16F10 tumor cells were transfected with mouse IL-18 siRNA (IL-18 Stealth Select RNAi (MSS205424, MSS205426) and control siRNA (Stealth RNAi Negative Control Med GC; Invitrogen) using HiPerFect reagent.

Microarray procedure using Illumina whole genome arrays

RNA was isolated from purified Kit$^+$ NK and Kit$^-$ NK cells as described (14). Biotin-labeled cRNA preparation was conducted using the Illumina TotalPrep RNA Amplification Kit (Applied Biosystems). cRNA (1.5 μg) was hybridized to the Illumina Sentrix BeadChip Mouse-6 V1 Array (Illumina) and scanned with an Illumina BeadStation 500×. For data collection, we used Illumina BeadStudio 3.1.1.0 software. Quantile normalization, statistical and bioinformatics analysis was conducted using the IlluminaGUI R-package (15).

MCMV infection

The Ly49H$^+$ congenic strain BALB.B6-CT8 (H-2^d, I-A^d, NK1.1$^+$, Ly49H$^+$) and the congenic Ly49H$^-$ strain BALB.B6-CT6 (H-2^d, I-A^d, NK1.1$^+$, Ly49H$^-$; ref. 16) were bred in the Animal Services Facility of the University of Western Australia (Nedlands, Western Australia, Australia). All mice were maintained in this facility during the course of infection. All animal experimentation was carried out with the approval of the Animal Ethics and Experimentation Committee of the University of Western Australia, according to the guidelines of the National Health and Medical Research Council. Mice were infected by intraperitoneal administration of 5×10^3 plaque-forming units (pfu) of salivary gland propagated MCMV-K181-Perth diluted in PBS-0.05% fetal calf serum (FCS). Control mice received PBS/0.05% FCS. Single-cell suspensions were prepared from spleen and cervical lymph nodes and cells preincubated on ice for 30 minutes with EDTA-SS-FCS containing 20% normal goat serum before staining with the indicated antibodies.

Statistical analyses

Results are expressed as means ± SEM or as ranges when appropriate. Aberrant values were excluded using Dixon test. Two groups were compared by the Mann–Whitney test. When the variables studied were not normally distributed, nonparametric statistical methods were used. When 3 or more groups

Published OnlineFirst March 16, 2012; DOI:10.1158/0008-5472.CAN-11-3379

were compared, the Kruskal–Wallis test was used. We evaluated statistical significance with Prism software (GraphPad Software, Inc.). *P* values <0.05 were considered as significant.

Results

Exogenous or tumor-derived IL-18 facilitates the accumulation of immature NK cells *in vivo*

We compared different schedules of recombinant mouse endotoxin-free IL-18 (rIL-18) administration for their ability to interfere against B16F10 lung metastases. rIL-18 boosted the establishment of B16F10 metastases when it was injected twice a week (11), whereas daily administration of rIL-18 reduced tumorigenesis (11, 17). Because B16F10 lung metastases are controlled by NK cells, we analyzed the phenotypic profile of immature and mature NK cell subsets in various lymphoid organs as defined previously (18). Biweekly administration of IL-18 augmented the proportions of Kit (CD117)-expressing cells among all $CD3^-NK1.1^+$ NK cells in all lymphoid organs (Fig. 1A and B, top) and also in lungs (Fig. 1C) as well as their absolute cell numbers (Fig. 1A–C, bottom) in both naive (Fig. 1) and tumor-bearing mice (not shown). It is of note that the IL-18–induced expansion of Kit^+ NK cells in lymphoid organs was inversely correlated with intratumoral Kit^- mature NK cells (11).

Because bioactive IL-18 is released from growing tumors and recirculates in the serum at low concentrations (11), we carried out the phenotypic characterization of NK cells from tumor-bearing mice, which revealed a consistent expansion of Kit-expressing NK cells (Kit^+ NK) in lymphoid tissues. This phenomenon was observed in different genetic backgrounds (C57Bl/6 in Fig. 1D and E, and BALB/c in Fig. 1G), in 3 different tumor models (B16F10 melanoma in Fig. 1D–F) in spontaneous melanomas arising in transgenic mice that express the *RET proto-oncogene* driven by the metallothionein promoter (ref. 11; Supplementary Fig. S1A and S1B), in BCR/ABL-induced chronic myeloid leukemia in Supplementary Fig. S1C, in CT26 colon carcinoma in Fig. 1G and Supplementary Fig. S1D, which were inoculated either intravenously (Fig. 1D, E, and G) or subcutaneously (Supplementary Fig. S1E), while applying different phenotypic definitions for NK cells ($CD3^-NK1.1^+$ cells in C57Bl/6 mice and $CD3^-CD49b^+$ cells in BALB/c mice). The absolute numbers of Kit^+ NK cells increased by approximately 2-fold during tumor progression. This increase concerned primary and secondary lymphoid tissues with an early increase in draining or nondraining lymph nodes at days 6 to 9 after intravenous injection of tumor cells (Fig. 1D) or in draining lymph nodes in subcutaneous tumor models (Supplementary Fig. S1E). The distribution of Kit^+ NK cells among distinct mouse NK cell subsets defined by the differential expression of CD27 and CD11b (18) revealed that approximately 70% of the Kit^+ NK cells accumulating in tumor-draining lymph nodes were $CD27^+CD11b^-$ (Fig. 1F). Indeed, the establishment of CT26 lung metastases was accompanied by an accumulation of Kit^+CD11b^- NK cells in the spleen (Fig. 1G) and in the peripheral lymph nodes (data not shown), a phenomenon also observed in naive mice treated with a biweekly schedule of rIL-18 (Supplementary Fig. S1G).

To establish a causal link between IL-18 released by tumor cells and lymphoid organ–resident Kit^+CD11b^- NK cells, we carried out the transfection of B16F10 tumor cells with 2 distinct IL-18 siRNAs, which reduced the capacity of tumor cells to produce bioactive IL-18 as previously described (11). Upon inoculation into mice, B16F10 engineered to express low levels of IL-18 failed to expand Kit^+ NK cells (Fig. 2A) and compromised B16F10 tumorigenesis (11). To further substantiate the decisive contribution of IL-18 to the tumor-driven differentiation of Kit^+ NK cells *in vivo*, we used saturating amounts of IL-18BP, a naturally occurring IL-18 antagonist (13), that successfully abolished the development of Kit^+ NK cells in lymph nodes and spleens in both B16F10 and CT26 lung metastases models (Fig. 2B and C and not shown) as well as compromised tumor progression (11).

We recently reported that the numbers of B16F10 metastases were decreased in $IL\text{-}18R^{-/-}$ or $MyD88^{-/-}$ mice, suggesting that B16F10 progression was dependent on the IL-18R/MyD88 signaling pathway of the host (11). When B16F10 tumor cells were injected into $IL\text{-}18R^{-/-}$ or $MyD88^{-/-}$ mice, they failed to increase the number of Kit^+ NK cells in lymph nodes (Fig. 2D) and spleens (not shown).

We further aimed at investigating the mechanism of Kit^+ NK cell expansion. *In vitro*, purified Kit^- NK cells from tumor-free mice acquired surface expression of c-Kit within 24 hours after stimulation with recombinant mouse IL-18 (rIL-18), but not with stem cell factor (SCF), rIL-2, or rIL-12 (Fig. 2E and not shown). IL-18 stimulated the transcription of *c-kit* in bulk cultures of NK cells (not shown). As we failed to detect a significant increase in bromodeoxyuridine (BrdUrd) incorporation into the expanding Kit^+ NK cell subset upon administration of IL-18 (Supplementary Fig. S2), these cells likewise arise from differentiation rather than proliferation. Indeed, IL-18 promoted predominantly the differentiation of the immature Kit^-CD27^+ NK cell subset into Kit^+ NK cells (Fig. 2F).

It is noteworthy that SCF, the ligand for the KIT receptor, did not synergize with IL-18 for the *ex vivo* conversion of Kit^- into Kit^+ NK cells (Supplementary Fig. S3A) and was not required for the IL-18–mediated differentiation of Kit^+ NK cells *in vivo* because IL-18 can induce Kit^+ NK cell differentiation in Kit-deficient (W/Wsh) mice (Supplementary Fig. S3B). Kit signaling did not appear to be involved in survival of Kit^+ NK cells in tumor-bearing mice because imatinib mesylate, a tyrosine kinase inhibitor that targets Kit, did not modulate the anti-apoptotic protein Bcl2 (Supplementary Fig. S3C).

In conclusion, the IL-18/IL-18R/MyD88 axis is involved in the expansion of Kit^+-expressing NK cells associated with tumor progression.

Kit^+CD11b^- NK cells mediate immunosuppressive functions in tumor settings

To determine whether Kit^+ NK cells might stimulate the metastatic dissemination of NK-controlled tumors, we comparatively assessed the potential of Kit^+ (mostly composed of the $CD11b^-$ fraction; Fig. 1F) compared with Kit^- NK cells to influence lung metastases upon adoptive transfer into C57Bl/6 mice injected with B16F10 melanoma cells (Fig. 3A, left) or BALB/c mice injected with CT26 colon carcinoma cells (Fig.

Published OnlineFirst March 16, 2012; DOI:10.1158/0008-5472.CAN-11-3379

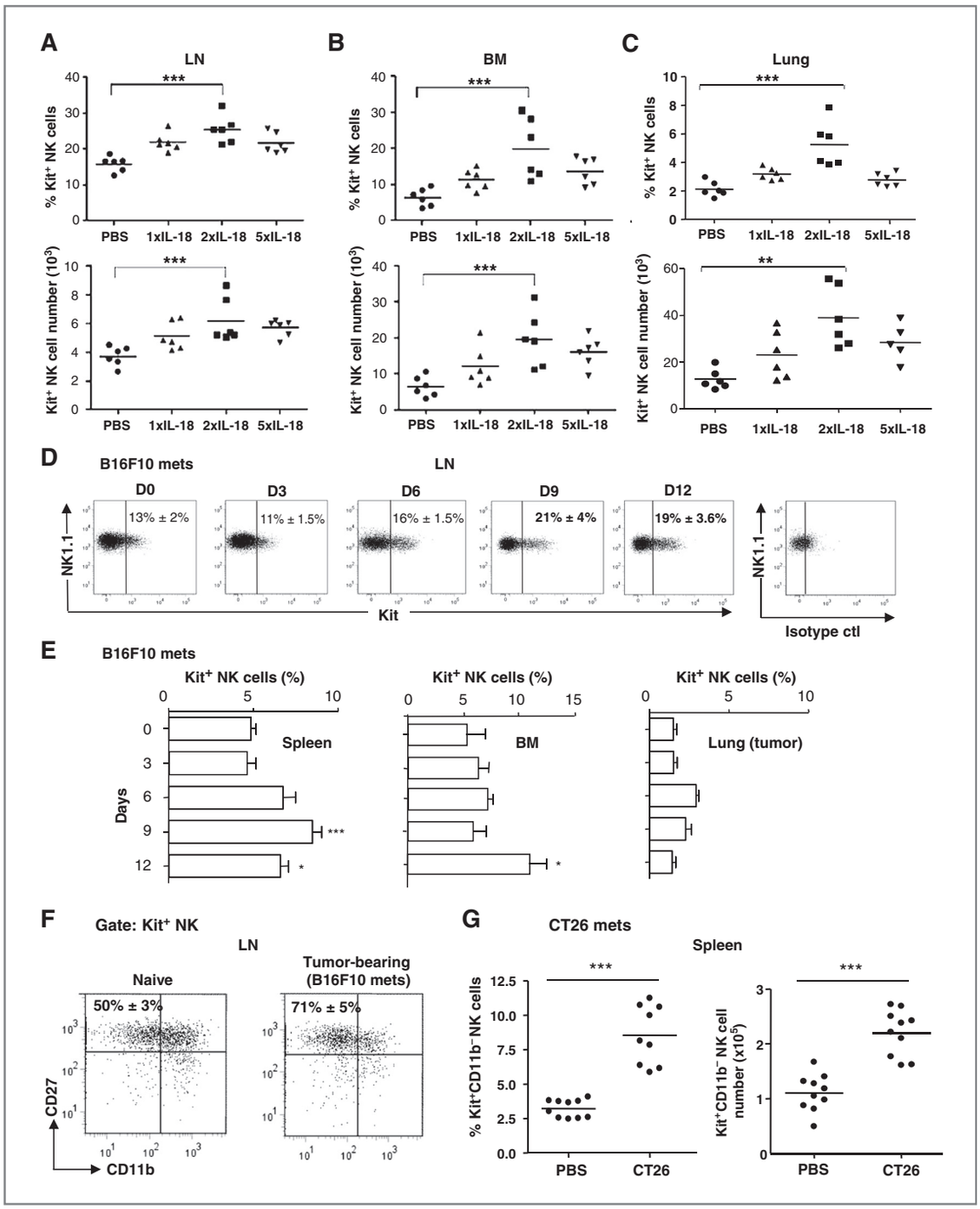

Figure 1. Low dose of IL-18 and tumor progression promote the accumulation of Kit$^+$CD11b$^-$ NK cells in lymphoid organs. A–C, expansion of Kit$^+$ NK cells during various schedules of rIL-18 administration. C57Bl/6 mice received rIL-18 i.p. (1 μg/inoculation) once on day 1 (1×), compared with twice on days 1 and 3 (2×), compared with 5 times (5×) on days 1 to 5. Percentages and/or absolute numbers of Kit$^+$ NK cells were determined in the lymph nodes (LN; A), the bone marrow (BM; B), and in the lungs (C) at day 7. The graph depicts the results for 6 animals in 2 independent experiments. The Kruskal–Wallis multiple comparison test was used for statistical analyses. **, $P < 0.01$; ***, $P < 0.001$ as compared with PBS group. D and E, accumulation of Kit$^+$ NK cells in lymphoid organs from C57Bl/6 mice bearing B16F10 metastases (mets). Single-cell suspensions were prepared from LN (D), spleen, bone marrow (BM), and tumor-bearing lungs (E) at various time points after i.v. inoculation of B16F10 cells. The percentage of Kit$^+$ NK cells (CD3$^-$NK1.1$^+$Kit/CD117$^+$) among all NK cells was determined. Flow cytometric analyses on LNs are shown in D for 1 representative experiment of 5 yielding similar results (means indicated in the top quadrant). The percentages of Kit$^+$ NK cells are shown in D as mean ± SEM of 5 independent experiments (including >3 mice per group). The Kruskal—Wallis multiple comparison test was used for statistical analyses. *, $P < 0.05$; ***, $P < 0.001$ as compared with day 0. F, CD27/CD11b expression on Kit$^+$ NK cells. Identical experimental setting as in C. Kit$^+$ NK cells were analyzed for their expression of CD27 and CD11b in lymph nodes of naive or tumor-bearing hosts at day 12. G, Kit$^+$CD11b$^-$ NK cells expand in CT26-bearing BALB/c mice. Proportion and absolute number of Kit$^+$CD11b$^-$ NK cells in spleens from CT26 metastases-bearing BALB/c mice. Data pooled from 3 independent experiments are presented. ***, $P < 0.001$ according to the Mann–Whitney test.

Published OnlineFirst March 16, 2012; DOI:10.1158/0008-5472.CAN-11-3379

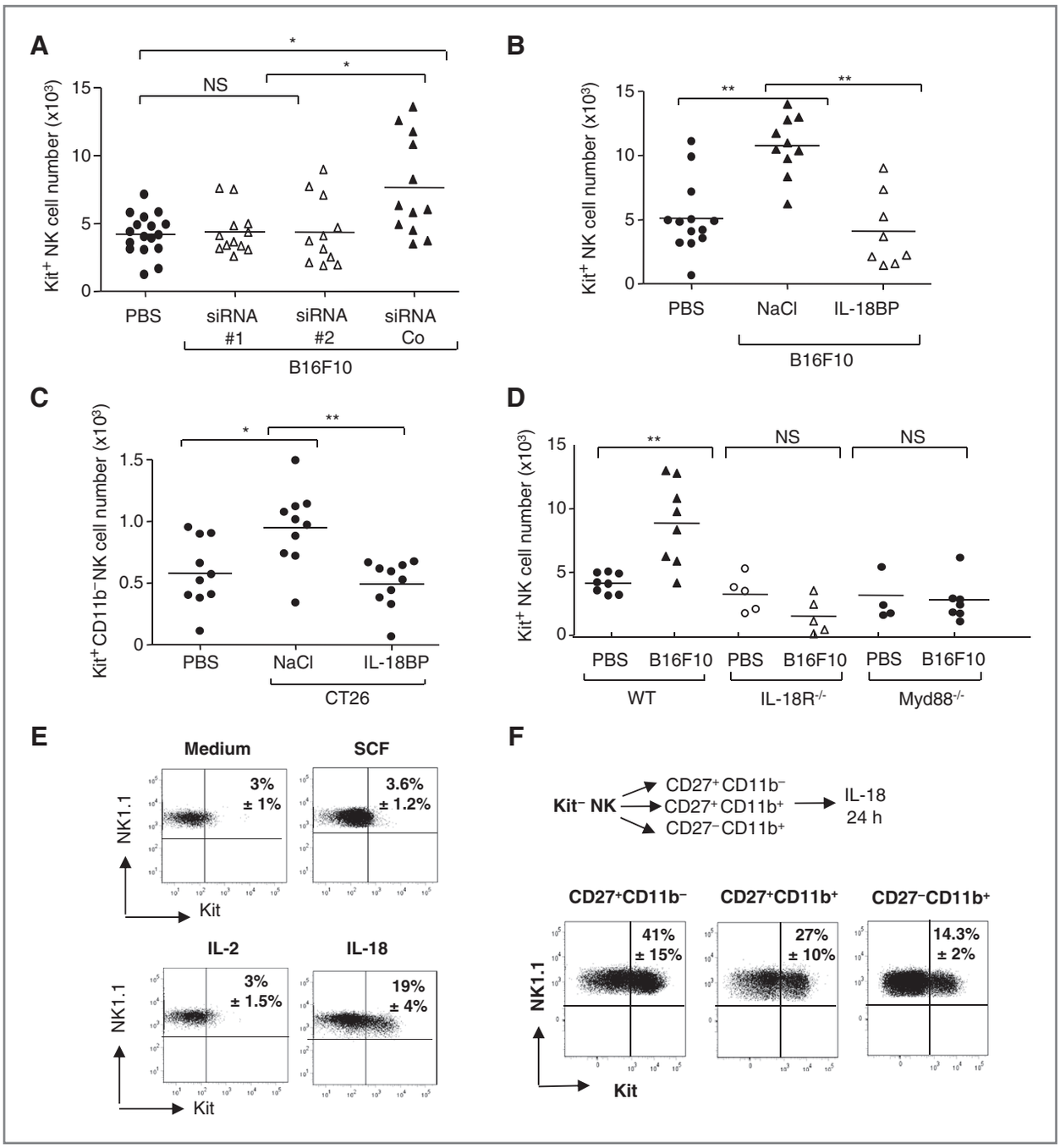

Figure 2. Tumor-driven IL-18 promotes the accumulation of Kit$^+$ NK cells in lymphoid organs. A, IL-18–dependent accumulation of Kit$^+$ NK cells in response to tumor inoculation. Flow cytometric analyses were conducted to determine the percentages and therefore the absolute numbers of Kit$^+$ NK cells in LNs at day 6 post-intravenous inoculation of B16F10 transfected with control siRNA (siRNA Co) or 2 different IL-18–depleting siRNAs (siRNA #1, #2). The graph depicts all the pooled data from 3 independent experiments with 3 to 5 mice per group. *, $P < 0.05$ according to the Kruskal–Wallis test. NS, not significant. B and C, pharmacologic neutralization of IL-18 by IL-18BP decreases Kit$^+$ NK cell expansion in various tumor models. IL-18BP was administered as described in Materials and Methods. The quantification of Kit$^+$ NK cells in LNs of C57Bl/6 mice inoculated with B16F10 (B) and BALB/c mice inoculated with CT26 (C) was conducted on day 9. The graph depicts the pooled results of 3 independent experiments containing at least 2 to 4 mice per group. *, $P < 0.05$; **, $P < 0.01$ according to the Kruskal–Wallis test. NS, not significant. D, IL-18R/MyD88-mediated host responsiveness is required for Kit$^+$ NK cell expansion. A total of 3×10^5 B16F10 were inoculated i.v. in wild-type (WT) versus IL-18R$^{-/-}$ or MyD88$^{-/-}$ mice. LN Kit$^+$ NK cells were enumerated on day 12. **, $P < 0.01$ according to the Kruskal–Wallis test. NS, not significant. E, IL-18 selectively induces the differentiation of Kit$^+$ NK cells *in vitro*. Kit$^-$ NK cells were stimulated with rmSCF (10 ng/mL), rhIL-2 (100,000 IU/mL), or rmIL-18 (25 ng/mL) overnight. Percentages of CD3$^-$NK1.1$^+$Kit$^+$ were determined by flow cytometry. One representative experiment of 3 is shown. F, IL-18 preferentially drives the CD27$^+$CD11b$^-$ subset of Kit$^-$ NK cells into Kit$^+$ NK cells. Cell-sorted Kit$^-$CD27$^+$CD11b$^-$ or Kit$^-$CD27$^+$CD11b$^+$ or Kit$^-$CD27$^-$CD11b$^+$ NK cell subsets were cultured overnight with IL-18 (25 ng/mL). The percentage of Kit expression after overnight culture was determined on CD3$^-$NK1.1$^+$ cells among these 3 different cultures. One representative experiment of 3 is shown and the mean ± SEM of percentages obtained in 3 experiments are indicated.

Published OnlineFirst March 16, 2012; DOI:10.1158/0008-5472.CAN-11-3379

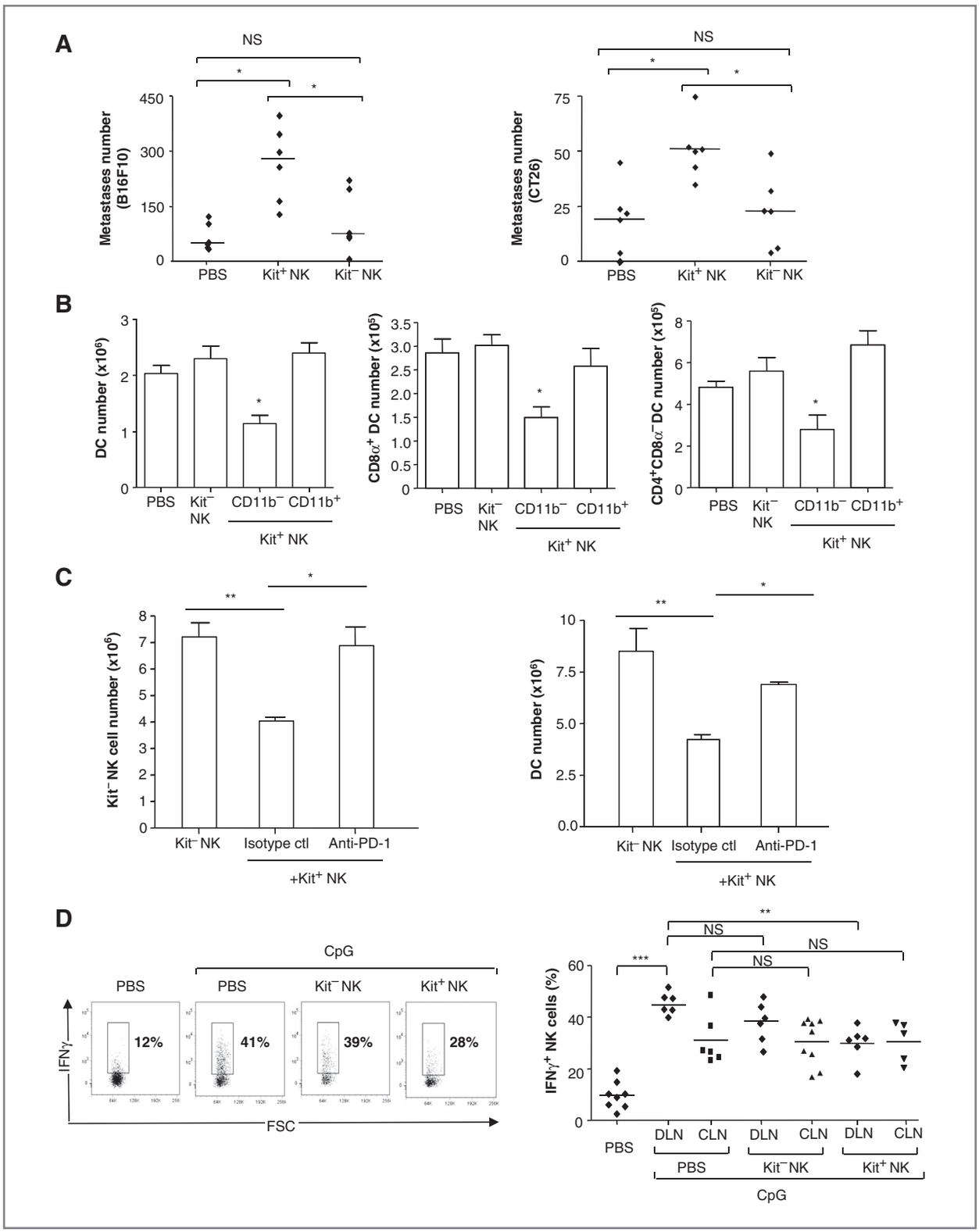

Figure 3. Kit$^+$CD11b$^-$ NK cells impair tumor immunosurveillance and TLR9 inflammation by targeting DCs and mature NK cell homeostasis. A, protumorigenic effect of Kit$^+$ NK cells. At day 0, C57Bl/6 (left) or BALB/c (right) mice were injected i.v. with 3×10^5 B16F10 or CT26 tumor cells, respectively. A total of 3×10^5 syngeneic Kit$^+$ or Kit$^-$ NK cells purified from spleens using magnetic purification procedure were adoptively transferred 2 days after tumor inoculation.

Published OnlineFirst March 16, 2012; DOI:10.1158/0008-5472.CAN-11-3379

3A, right). In both cases, Kit$^+$ (but not Kit$^-$) NK cells promoted the establishment of lung metastases (Fig. 3A).

Interestingly, the adoptive transfer of Kit$^+$CD11b$^-$ NK cells (but not Kit$^-$ NK cells) could eliminate part of the DC pool *in vivo*, depleting both CD8α$^+$ and CD11b$^+$ spleen- or lung-resident DCs (Fig. 3B). Considering the critical role of DCs in maintaining the NK cell homeostasis (19), it was not surprising to observe that upon adoptive transfer into athymic C57Bl/6 nude mice, Kit$^+$ NK lymphocytes also reduced the absolute number of Kit$^-$ NK cells both in the spleen (Fig. 3C) and in the lungs (data not shown). Because DCs play a key role in controlling NK cell activation (20), a reduction of the DC/NK cell pool could have functional consequences during stimulation with Toll-like receptor (TLR)9 agonists. We monitored the effects of a systemic adoptive transfer of Kit$^+$ NK cells in lymph nodes, draining a CpG ODN–driven inflammation. Kit$^+$ (but not Kit$^-$) NK cells induced a significant decrease in the proportion of IFNγ-producing NK cells in the lymph node draining the TLR9L-induced inflammation (Fig. 3D).

Altogether, Kit$^+$CD11b$^-$ NK cells are endowed with immunosuppressive functions.

B7-H1 is overexpressed on Kit$^+$ NK cells

Cell-sorted splenic CD3$^-$NK1.1$^+$ Kit$^+$ cells from tumor-bearing mice that were NKp46$^+$, CD49b$^+$, and CD122$^+$ (Supplementary Fig. S4) expressed higher levels of CXCR3 (Supplementary Fig. S4) than CD3$^-$NK1.1$^+$Kit$^-$ cells. Three independent microarray-based comparisons of fluorescence-activated cell-sorting (FACS)-purified CD3$^-$NK1.1$^+$Kit$^+$ and CD3$^-$NK1.1$^+$Kit$^-$ cells revealed profound differences in the transcriptome of the 2 NK cell subsets (Fig. 4A, left; Supplementary Tables S1 and S2) that could be further confirmed at the protein level for several gene products (Fig. 4A, right). CD3$^-$NK1.1$^+$Kit$^+$ overexpressed 4 genes with potential immunosuppressive properties by a factor of >2.5: (i) Lag3, which is a marker of regulatory T cells (21); (ii) heme-oxygenase (HO-1), which inhibits the rejection of heart allografts (22); (iii) CTLA4, which inhibits CD28-dependent costimulation of T cells (23); and (iv) B7-H1 (PDL-1, CD274), which stimulates the PD-1 death receptor on activated T lymphocytes (ref. 24; Fig. 4A, top right). The immunofluorescence-detectable expression of B7-H1 was significantly higher on the surface of Kit$^+$ NK than on Kit$^-$ NK cells in all lymphoid compartments (Fig. 4B, top). No significant phenotypic differences between Kit$^+$ NK cells sorted from naive compared with tumor-bearing hosts could be observed except for a substantial enhancement of B7-H1 expression in tumor bearers (Fig. 4B, bottom). Moreover, rIL-18 could induce B7-H1 expression on the immature Kit$^-$CD27$^+$CD11b$^-$ NK cell subset differentiating into Kit$^+$ NK cells (Fig. 4C).

Kit$^+$CD11b$^-$ NK cells mediate their immunoablative functions in a B7-H1–dependent fashion

We showed that the adoptive transfer of Kit$^+$CD11b$^-$ NK cells in naive mice was accompanied by a reduction of the DC pool (Fig. 3B). The Kit$^+$ NK–mediated DC depletion appeared to be a direct effect, as Kit$^+$ NK cells could kill immature but not maturing/activated bone marrow–derived DCs *in vitro* (Fig. 5A and B). Killing of immature DCs was observed only after cocultures of DCs with Kit$^+$ NK cells but not Kit$^-$ NK counterparts (AnnexinV$^+$ DC in DC + Kit$^-$ NK cells: 10.7% ± 3.6% vs. AnnexinV$^+$ DC in DC + Kit$^+$ NK cells: 34% ± 4.1%, $P = 0.02$) and was abrogated in the presence of neutralizing anti-B7-H1 but not anti-Lag3 antibodies (Fig. 5C). In line with these observations, the contraction of DCs induced by Kit$^+$ NK cells (Fig. 3B) was abolished by injection of an anti-PD-1–blocking antibodies *in vivo* (Fig. 3C, right), suggesting that B7-H1 present on Kit$^+$ NK cells depleted PD-1–expressing DC, compromising indirectly the DC-mediated mature NK cell homeostasis in lymphoid organs (Fig. 3C, left). Importantly, preincubation of Kit$^+$ NK cells with neutralizing anti-B7-H1 antibody before adoptive transfer into B16F10 tumor–bearing mice abolished the metastasis-enhancing effect of Kit$^+$ NK cells (Fig. 5D).

Kit$^+$ NK cells accumulated not only in the context of a tumor but also in MCMV infection

Accumulation of Kit$^+$ NK cells was also observed during the NK cell–controlled MCMV infection. The frequency and number of Kit$^+$ NK cells were monitored over time after MCMV infection in MCMV-susceptible (BALB.B6-CT6) and -resistant (BALB.B6-CT8) mouse strains (16). Kit$^+$ NK cell accumulation was maximal in MCMV-resistant BALB.B6-CT8 mice, in both the spleens and cervical lymph nodes (Fig. 6). Although Ly49H$^+$ NK cells are essential to limit MCMV during the acute stage of infection, their expansion occurs later during infection and those cells are Kit$^-$ (25, 26). Like cancer-induced Kit$^+$ NK cells, MCMV-induced Kit$^+$ NK cells also overexpressed Lag3 and 2B4

Quantification of lung metastases was carried out at day 12. Data pooled from 2 experiments with 3 mice per group are shown. The Kruskal–Wallis multiple comparison test was used for statistical analyses. *, $P < 0.05$. NS, not significant. B, transient depletion of spleen resident DC subsets after adoptive transfer of Kit$^+$CD11b$^-$ NK cells in WT mice. About 10^5 purified Kit$^+$CD11b$^-$ or CD11b$^+$ NK and Kit$^-$ NK cells were adoptively transferred into C57Bl/6 mice. The absolute numbers of DCs (CD11c$^+$/I-Ab$^+$ cells; left) and among those the CD8α$^+$ DC subset (middle) or the CD4$^+$CD8 α$^-$ DC subset (right) residing in spleens or lungs (not shown) were determined at 48 hours by enumerating cells in trypan blue exclusion assays combined to 6 color staining and flow cytometry. The data pooled from 3 independent experiments are shown. Kruskal–Wallis test was used for statistical analyses and significant effects are indicated with asterisks. C, Kit$^+$ NK cells eliminate DCs and Kit$^-$ NK cells *in vivo* in a PD-1–dependent manner. A total of 3×10^5 purified Kit$^+$ or Kit$^-$ NK cells was adoptively transferred into nude C57Bl/6 mice. Blocking anti-PD-1 (or isotype control) antibody was injected i.p. as described in Materials and Methods. Absolute numbers of DC (CD11c$^+$/CMH Class II$^+$) and Kit$^-$ NK (CD3$^-$NK1.1$^+$CD117$^-$) cells were determined in spleen at 48 hours by flow cytometry. The graph shows the data from 2 independent experiments with 2 to 4 mice per group. D, Kit$^+$ NK cells keep in check IFNγ-producing NK cells during TLR9L-induced inflammation. A total of 5×10^5 Kit$^+$ or Kit$^-$ NK cells were adoptively transferred i.v. into naive C57Bl/6 mice, 6 hours after footpad inoculation of 10 μg of CpG ODN 1668. Mice were sacrificed at 18 hours after NK cell transfer to assess the proportion of IFNγ-producing CD3$^-$NK1.1$^+$ NK cells in the draining (DLN) and controlateral (CLN) lymph nodes. The data pooled from 3 independent experiments are shown (each dot representing one mouse). **, $P < 0.01$; ***, $P < 0.001$. Ctl, control; FSC, forward scatter.

Published OnlineFirst March 16, 2012; DOI:10.1158/0008-5472.CAN-11-3379

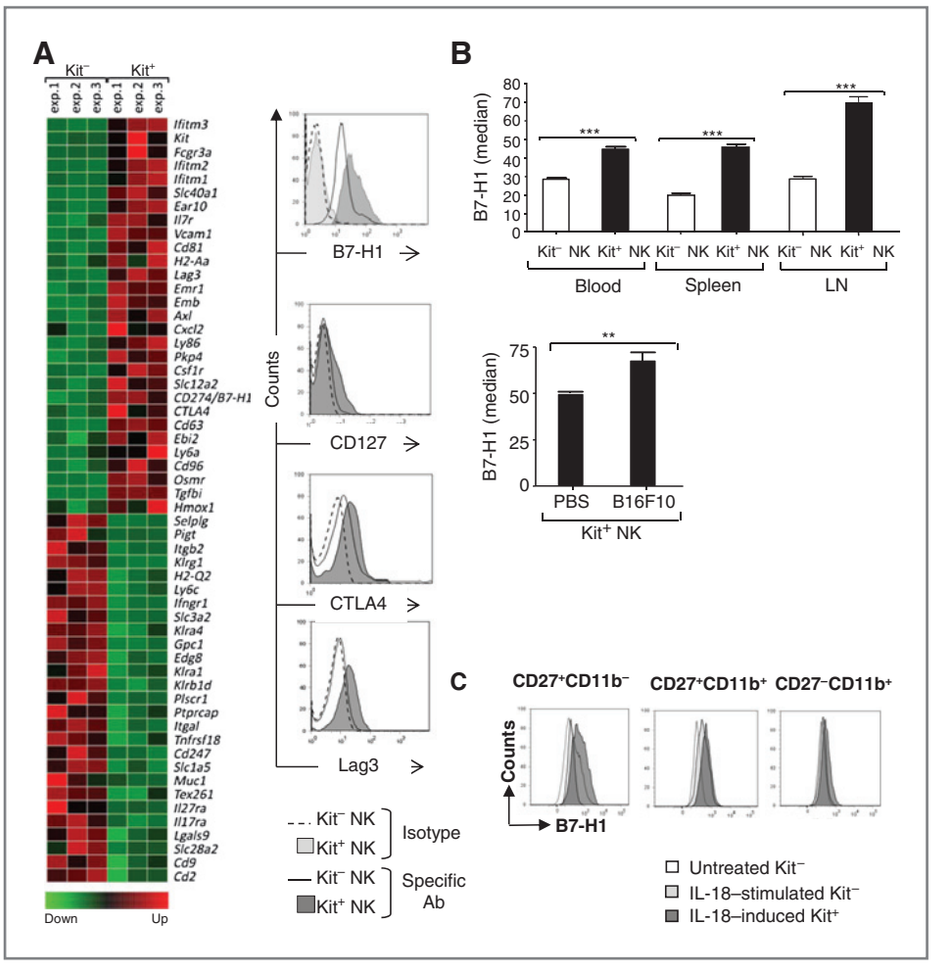

Figure 4. Phenotypic characterization of Kit$^+$ NK cells. A, transcriptional profile of Kit$^+$ versus Kit$^-$ NK cells. The heatmap details 28 genes elevated in Kit$^+$ NK cells [fold change (FC) = 2.5, $P < 0.05$] and 28 genes elevated in Kit$^-$ NK cells (FC = 2.5, $P < 0.05$). Shown are row-wise z-transformed intensity values (mean = 0, SD = 1) with high-intensity values shown in red and low-intensity values shown in green. Representative histograms of fluorescence intensities for B7-H1, CD127, CTLA4, and Lag3 in Kit$^+$ versus Kit$^-$ NK cells from naive LNs are depicted. Microarray data have been submitted to GEO database under GSE9431. B, expression of B7-H1 molecules on NK cells. Medians of fluorescence intensities of B7-H1 on NK cells in various locations in naive mice (top) versus tumor bearers (bottom) are depicted as mean ± SEM of 3 independent experiments. C, IL-18 preferentially drives the CD27$^+$CD11b$^-$ subset of Kit$^-$ NK cells into B7-H1$^+$ NK cells. Same experimental setting as in Fig. 2F but B7-H1 surface expression was analyzed. One representative analysis of 3 is shown. Among IL-18–induced Kit$^+$ NK cells, the median of B7-H1 expression of CD27$^+$CD11b$^-$ and of CD27$^+$CD11b$^+$ is 1,512 and 648, respectively. For statistics in all graphs, **, $P < 0.01$; ***, $P < 0.001$ according to the Mann–Whitney test.

and were CD11b$^-$ (not shown). B7-H1 expression on Kit$^+$ NK cells increased slightly, peaking at day 6 postinfection in the Kit$^+$ fraction of NK cells especially in the lymph nodes (Fig. 6). Therefore, Kit$^+$ NK cells may represent a novel innate lymphoid subset exerting immunoregulatory functions in NK cell–dependent cancers but also in infections.

Discussion

Although the counter-regulation of the T-cell arm of immunity by suppressor T cells has been widely investigated, the regulatory activity of innate effectors has not been thoroughly explored in the context of tumors (27). NK cells can produce immunosuppressive cytokines that modulate immune responses (28). Even more overlooked is the potential counter-regulation of NK cells by NK cells (29). Here we show for the first time that tumor-derived IL-18 can expand a subset of NK cells that express the c-kit receptor. This NK cell subset circulates in the blood stream and resides in primary and secondary lymphoid organs (Fig. 1, Supplementary Fig. S1 and data not shown) and can deplete the peripheral pool of DCs. Because DCs are involved in the NK cell activation and homeostasis, this mechanism can, at least in part, contribute to NK cell–based immunosuppression and tumor outgrowth. We showed that this NK cell subset regulates innate NK cell functions (as shown in the manuscript in cancer and CpG ODN–mediated inflammation).

The data presented here suggest that an NK cell subset could act as a negative regulator of the DC/NK cell responses (Fig. 3A, C, and D). Kit$^+$ NK cells represent about 3.3% ± 0.7% of blood, 1.23% ± 0.5% of lung, 4.8% ± 1.4% of spleen, 13.2% ± 2.4% of lymph node, and 5.4% ± 1.8% of bone marrow NK cells in naive

Published OnlineFirst March 16, 2012; DOI:10.1158/0008-5472.CAN-11-3379

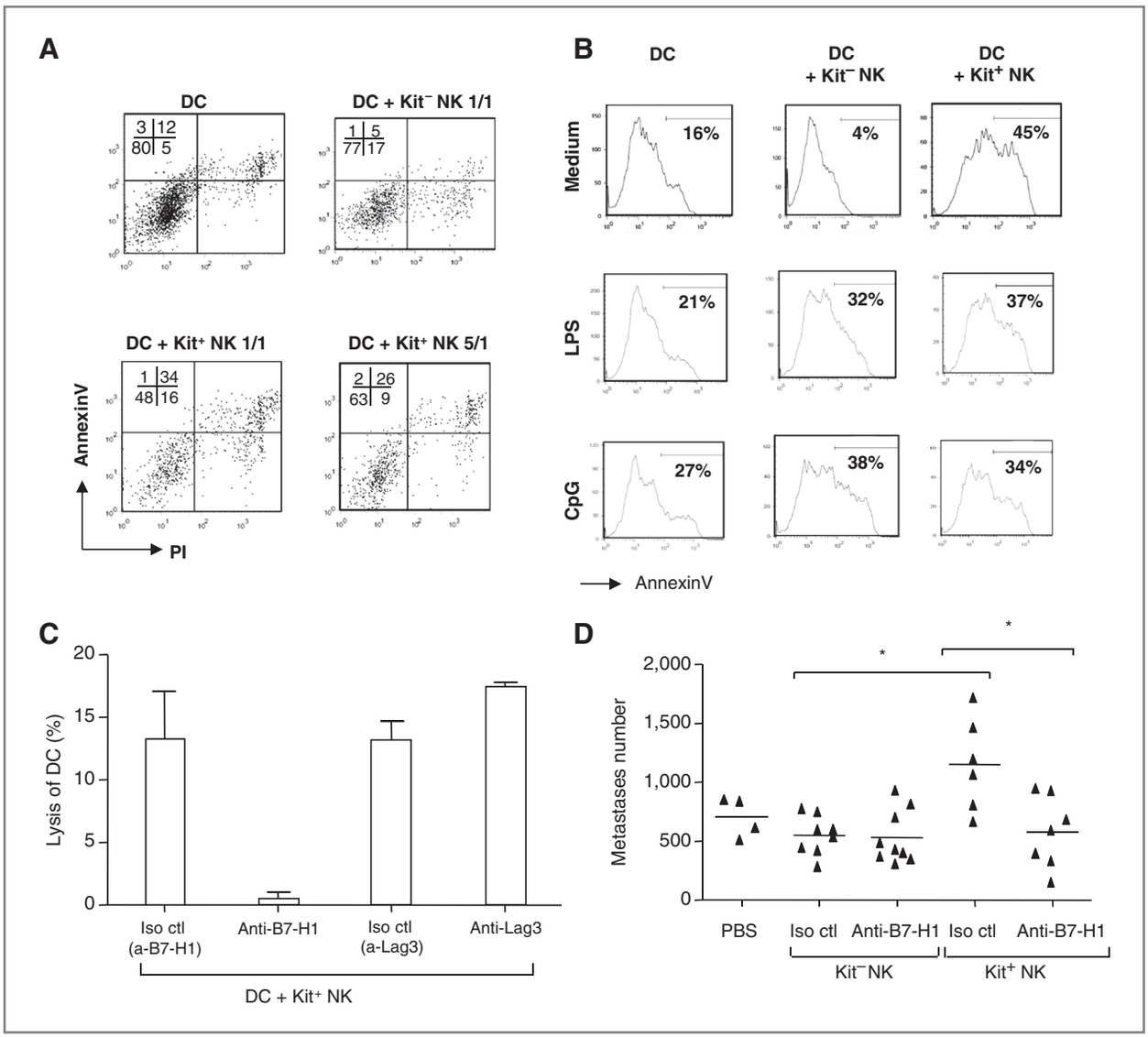

Figure 5. Kit$^+$ NK cells can kill immature DCs through a B7-H1–dependent manner. A and B, direct killing of immature DCs by Kit$^+$ but not Kit$^-$ NK cells *in vitro*. *In vitro* cocultures of Kit$^+$ NK cells with immature bone marrow–derived DC (derived in granulocyte macrophage colony—stimulating factor), or lipopolysaccharide- or CpG-matured BM DCs at a 1/1 or 5/1 DC/NK ratio were examined in flow cytometry for AnnexinV/propidium iodide (PI) expression. Analysis was conducted on CD11c$^+$/I-Ab$^+$ cells. Representative dot plots (A) or histograms (B) are shown in each condition of coculture. The experiments have been conducted 3 times with identical results. C, same experimental setting as in A, but adding neutralizing anti-B7-H1 (10 μg/mL) or anti-Lag3 antibodies (10 μg/mL) in the coculture. Percentage of killed DCs was determined by flow cytometry using AnnexinV/7-aminoactinomycin D (AAD) staining. Percentage of DC lysis was calculated as follows: [(% killed DCs in test) − (% killed DC in DC alone)]/(% killed DC in DC alone) × 100. Means ± SEM of percentages obtained in 3 experiments are indicated. D, B7-H1–mediated prometastatic activity of Kit$^+$ NK cells on the B16F10 melanoma. A total of 3×10^5 Kit$^+$ or Kit$^-$ NK cells were preincubated with saturating amounts of neutralizing anti-B7-H1 or isotype (iso) control (ctl) antibody (Ab) and washed before adoptive transfer in B16F10-bearing mice. *, $P < 0.05$ according to the Kruskal–Wallis test.

animals (Fig. 1). In tumor-bearing animals, the percentages and absolute numbers of Kit$^+$ NK cells increased (Fig. 1) to levels that mediate inhibitory effects on the DC/NK cell cross-talk. The adoptive transfer of Kit$^+$ NK cells could promote the outgrowth of B16F10 melanoma and CT26 colon carcinoma cells (Fig. 3A) and reduce CpG-induced NK cell IFNγ secretion (Fig. 3D). In the context of a tumor, Kit$^+$ NK cell accumulation is dependent on tumor-derived IL-18 that induces a conversion of Kit$^-$ NK cells into Kit$^+$ B7-H1$^+$ NK cells. Kit$^+$ NK cells did not rely on the c-Kit pathway for their conversion (Fig. 2E; Supplementary Fig. S3A and S3B), B7-H1 expression (Supplementary Fig. S3D), or survival (Supplementary Fig. S3C). These Kit$^+$ NK cells expressed higher levels of B7-H1 than in Kit$^-$ NK cells. Saudemont and colleagues described the capacity of Cxcl10 to induce B7-H1 expression on spleen NK cells, which was associated with the NK cell–dependent control of minimal residual disease in leukemia (30). In tumor- or IL-18–dependent experimental settings, Cxcl10 is not upregulated in spleen (11),

Published OnlineFirst March 16, 2012; DOI:10.1158/0008-5472.CAN-11-3379

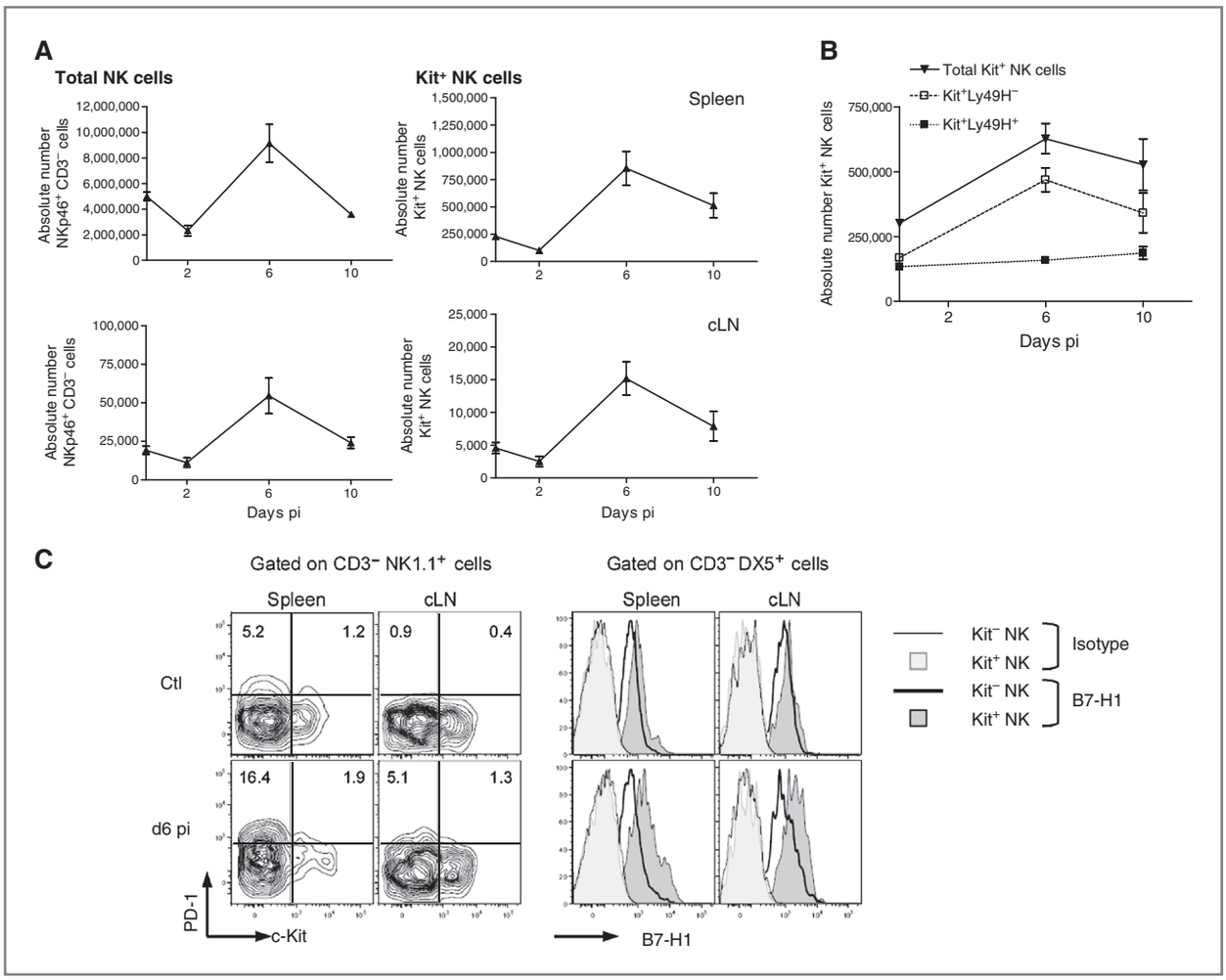

Figure 6. Accumulation of Kit$^+$ NK cells during MCMV infection in resistant mice. A, spleen and cervical (CLN) lymph nodes were collected from MCMV-resistant (BALB.B6-CT8) mice infected with 5×10^3 pfu of MCMV-K181 for 0, 2, 6, and 10 days and absolute numbers of NK cells enumerated. The number of c-Kit$^+$ NK cells was also determined. Data from spleen and cLNs are shown. B, numbers of splenic c-Kit$^+$ NK cells within the total NK cell pool as well as the Ly49H$^-$ and Ly49H$^+$ NK cell subpopulations were determined at the indicated times after infection. C, NK cells isolated from the spleen and cLNs were collected from uninfected control (ctl) mice or MCMV-infected (day 6 pi) mice and analyzed for c-Kit, PD-1, and B7-H1 expression. Isotype control antibodies were used to determine the fluorescence background, as indicated. Values indicate the percentage of cells in the indicated gates and quadrants. pi, postinjection.

whereas CXCR3 expression (at the transcriptional and protein levels) is superior in Kit$^+$ than in Kit$^-$ NK cells. These observations suggest that the functional outcome of IL-18 compared with Cxcl10 on NK cell triggering may be different.

Intriguingly, IL-18, a key defense cytokine that plays a central role in inflammation and immune responses (17, 31), represented a major immunosuppressant capable of electively promoting the conversion of Kit$^-$CD27$^+$CD11b$^-$ NK cells into regulatory B7-H1$^+$ Kit$^+$ NK cells *in vitro* and *in vivo* (Fig. 1A and B; Supplementary Figs. S1G, S2E, S2F, and S4C). In addition, as shown here, IL-18 mediates immunosuppression on innate immunity (Fig. 2). The 2-weekly schedule of IL-18 administration accelerated tumor progression (11), at least in part, through the induction of Kit$^+$ NK cells (Fig. 1A and B), in contrast to daily administration of IL-18, which induced inflammation (IL-15, CCR4, CCL5, IL-1β, IL-12p40) leading to antitumor responses (11). IL-18 could drive the differentiation of immature CD27$^+$CD11b$^-$ NK cells into c-Kit- and B7-H1–overexpressing cells (Fig. 4C). Moreover, the prometastatic effects of recombinant IL-18 involved the B7-H1/PD-1 pathway because anti-PD-1 antibodies reduced the IL-18–mediated tumor progression (11) and the protumorigenic effects of IL-18–associated Kit$^+$ NK cells were significantly blunted by anti-B7-H1–neutralizing antibodies (Fig. 5D).

The identification of the human ortholog of mouse Kit$^+$CD11b$^-$ NK cells and of causal links between IL-18 and the B7-H1/PD-1 pathways in human malignancies remains important challenge of the future development of antibodies blocking immune tolerance checkpoints.

Disclosure of Potential Conflicts of Interest

No potential conflicts of interest were disclosed.

Published OnlineFirst March 16, 2012; DOI:10.1158/0008-5472.CAN-11-3379

Authors' Contributions

Conception and design: M. Terme, L. Aymeric, J. Coudert, M. Degli-Esposti, L. Zitvogel
Development of methodology: E. Ullrich, K. Meinhardt, F. Ghiringhelli, B. Ryffel, H. Yagita, L. Zitvogel
Acquisition of data (provided animals, acquired and managed patients, provided facilities, etc.): M. Terme, E. Ullrich, L. Aymeric, K. Meinhardt, M. Desbois, F. Ghiringhelli, H. Yagita, L. Chen, S. Mecheri, A. Prevost-Blondel, M. Degli-Esposti
Analysis and interpretation of data (e.g., statistical analysis, biostatistics, computational analysis): M. Terme, E. Ullrich, L. Aymeric, K. Meinhardt, J. Coudert, M. Desbois, G. Kaplanski, J.L. Schultze, E. Tartour, G. Kroemer, M. Degli-Esposti, L. Zitvogel
Writing, review, and/or revision of the manuscript: M. Terme, K. Meinhardt, S. Viaud, H. Yagita, L. Chen, J.L. Schultze, G. Kroemer, M. Degli-Esposti, L. Zitvogel
Administrative, technical, or material support (i.e., reporting or organizing data, constructing databases): S. Viaud, B. Ryffel, H. Yagita, M. Kato, L. Zitvogel
Study supervision: L. Zitvogel
IL-18BP expertise: G. Kaplanski
Data dealing with MCMV infection: Degli-Esposti
Participate in scientific discussions concerning this topic: N. Chaput

Acknowledgments

The authors thank Y. Lecluse, D. Metivier, and P. Rameau for cell sorting.

Grant Support

This work was supported by INCa, ANR, Ligue contre le cancer (équipes labellisées de L. Zitvogel and G. Kroemer) and INFLACARE EU grant. M. Terme was supported by Cancéropôle IDF and the Ligue Nationale contre le Cancer. E. Ullrich and K. Meinhardt were supported by the Deutsche Forschungsgemeinschaft (DFG), the Deutsche Krebshilfe (German Cancer Aid), the ELAN and IZKF program of the University Erlangen, Germany. L. Aymeric was supported by the Institut National du Cancer (INCa), and the Association pour la Recherche sur le Cancer (ARC).

The costs of publication of this article were defrayed in part by the payment of page charges. This article must therefore be hereby marked *advertisement* in accordance with 18 U.S.C. Section 1734 solely to indicate this fact.

Received October 14, 2011; revised February 13, 2012; accepted February 22, 2012; published OnlineFirst March 16, 2012.

References

1. Nishikawa H, Jager E, Ritter G, Old LJ, Gnjatic S. CD4+ CD25+ regulatory T cells control the induction of antigen-specific CD4+ helper T cell responses in cancer patients. Blood 2005;106:1008–11.
2. Chen ML, Pittet MJ, Gorelik L, Flavell RA, Weissleder R, von Boehmer H, et al. Regulatory T cells suppress tumor-specific CD8 T cell cytotoxicity through TGF-beta signals *in vivo*. Proc Natl Acad Sci U S A 2005;102:419–24.
3. Vivier E, Ugolini S. Regulatory natural killer cells: new players in the IL-10 anti-inflammatory response. Cell Host Microbe 2009;6:493–5.
4. Zhang C, Zhang J, Tian Z. The regulatory effect of natural killer cells: do "NK-reg cells" exist? Cell Mol Immunol 2006;3:241–54.
5. Shibatomi K, Ida H, Yamasaki S, Nakashima T, Origuchi T, Kawakami A, et al. A novel role for interleukin-18 in human natural killer cell death: high serum levels and low natural killer cell numbers in patients with systemic autoimmune diseases. Arthritis Rheum 2001;44:884–92.
6. Mazodier K, Marin V, Novick D, Farnarier C, Robitail S, Schleinitz N, et al. Severe imbalance of IL-18/IL-18BP in patients with secondary hemophagocytic syndrome. Blood 2005;106:3483–9.
7. Dinarello CA. Interleukin-18. Methods 1999;19:121–32.
8. Dinarello CA. The paradox of pro-inflammatory cytokines in cancer. Cancer Metastasis Rev 2006;25:307–13.
9. Taieb J, Chaput N, Menard C, Apetoh L, Ullrich E, Bonmort M, et al. A novel dendritic cell subset involved in tumor immunosurveillance. Nat Med 2006;12:214–9.
10. Zhou P, L'Italien L, Hodges D, Schebye XM. Pivotal roles of CD4+ effector T cells in mediating agonistic anti-GITR mAb-induced-immune activation and tumor immunity in CT26 tumors. J Immunol 2007;179:7365–75.
11. Terme M, Ullrich E, Aymeric L, Meinhardt K, Desbois M, Delahaye N, et al. IL-18 induces PD-1-dependent immunosuppression in cancer. Cancer Res 2011;71:5393–9.
12. Azuma T, Yao S, Zhu G, Flies AS, Flies SJ, Chen L. B7-H1 is a ubiquitous antiapoptotic receptor on cancer cells. Blood 2008;111:3635–43.
13. Dinarello CA. Targeting interleukin 18 with interleukin 18 binding protein. Ann Rheum Dis 2000;59 Suppl 1:i17–20.
14. Debey S, Schoenbeck U, Hellmich M, Gathof BS, Pillai R, Zander T, et al. Comparison of different isolation techniques prior gene expression profiling of blood derived cells: impact on physiological responses, on overall expression and the role of different cell types. Pharmacogenomics J 2004;4:193–207.
15. Schultze JL, Eggle D. IlluminaGUI: graphical user interface for analyzing gene expression data generated on the Illumina platform. Bioinformatics 2007;23:1431–3.
16. Scalzo AA, Brown MG, Chu DT, Heusel JW, Yokoyama WM, Forbes CA. Development of intra-natural killer complex (NKC) recombinant and congenic mouse strains for mapping and functional analysis of NK cell regulatory loci. Immunogenetics 1999;49:238–41.
17. Smyth MJ, Swann J, Kelly JM, Cretney E, Yokoyama WM, Diefenbach A, et al. NKG2D recognition and perforin effector function mediate effective cytokine immunotherapy of cancer. J Exp Med 2004;200:1325–35.
18. Hayakawa Y, Smyth MJ. CD27 dissects mature NK cells into two subsets with distinct responsiveness and migratory capacity. J Immunol 2006;176:1517–24.
19. Mortier E, Advincula R, Kim L, Chmura S, Barrera J, Reizis B, et al. Macrophage- and dendritic-cell-derived interleukin-15 receptor alpha supports homeostasis of distinct CD8+ T cell subsets. Immunity 2009;31:811–22.
20. Lucas M, Schachterle W, Oberle K, Aichele P, Diefenbach A. Dendritic cells prime natural killer cells by trans-presenting interleukin 15. Immunity 2007;26:503–17.
21. Huang CT, Workman CJ, Flies D, Pan X, Marson AL, Zhou G, et al. Role of LAG-3 in regulatory T cells. Immunity 2004;21:503–13.
22. Bach FH. Heme oxygenase-1 and transplantation tolerance. Hum Immunol 2006;67:430–2.
23. Zang X, Allison JP. The b7 family and cancer therapy: costimulation and coinhibition. Clin Cancer Res 2007;13:5271–9.
24. Chen L. Co-inhibitory molecules of the B7-CD28 family in the control of T-cell immunity. Nat Rev Immunol 2004;4:336–47.
25. Dokun AO, Chu DT, Yang L, Bendelac AS, Yokoyama WM. Analysis of *in situ* NK cell responses during viral infection. J Immunol 2001;167:5286–93.
26. Andrews DM, Scalzo AA, Yokoyama WM, Smyth MJ, Degli-Esposti MA. Functional interactions between dendritic cells and NK cells during viral infection. Nat Immunol 2003;4:175–81.
27. Johansson S, Berg L, Hall H, Hoglund P. NK cells: elusive players in autoimmunity. Trends Immunol 2005;26:613–8.
28. Mehrotra PT, Donnelly RP, Wong S, Kanegane H, Geremew A, Mostowski HS, et al. Production of IL-10 by human natural killer cells stimulated with IL-2 and/or IL-12. J Immunol 1998;160:2637–44.
29. Taniguchi RT, Guzior D, Kumar V. 2B4 inhibits NK-cell fratricide. Blood 2007;110:2020–3.
30. Saudemont A, Jouy N, Hetuin D, Quesnel B. NK cells that are activated by CXCL10 can kill dormant tumor cells that resist CTL-mediated lysis and can express B7-H1 that stimulates T cells. Blood 2005;105:2428–35.
31. Mailliard RB, Alber SM, Shen H, Watkins SC, Kirkwood JM, Herberman RB, et al. IL-18-induced CD83+CCR7+ NK helper cells. J Exp Med 2005;202:941–53.